

## Electromagnetic dissociation of Pb nuclei in peripheral ultrarelativistic heavy-ion collisions

Mario Vidović

*Institut für Theoretische Physik, Johann Wolfgang Goethe-Universität, Postfach 111 932,  
D-60054 Frankfurt am Main, Germany*

*and Gesellschaft für Schwerionenforschung (GSI), Planckstrasse 1, Postfach 110 552, D-64220 Darmstadt, Germany*

Martin Greiner

*Department of Physics, University of Arizona, Tucson, Arizona 85721*

Gerhard Soff

*Gesellschaft für Schwerionenforschung (GSI), Planckstrasse 1, Postfach 110 552, D-64220 Darmstadt, Germany*

(Received 20 May 1993)

We calculate the total electromagnetic dissociation cross section in peripheral heavy-ion collisions  $^{208}\text{Pb} + ^{208}\text{Pb}$  for the planned colliders the Brookhaven Relativistic Heavy Ion Collider, the CERN Large Hadron Collider, and the Superconducting Super Collider. The two nuclei interact via their Lorentz contracted electromagnetic fields leading to nuclear disintegration. We employ an impact-parameter-dependent version of the equivalent photon method with experimental photon-nucleus dissociation cross sections. The hadronic structure of the photon at large equivalent photon energies has been taken into account. In particular, we stress unitarity conservation of the dissociation probability for small impact parameters.

PACS number(s): 25.75.+r

The planned heavy-ion colliders RHIC (Brookhaven Relativistic Heavy Ion Collider), LHC (Large Hadron Collider) at CERN, and SSC (Superconducting Super Collider) in Texas will open exciting possibilities for fundamental physical studies. Besides the formation of a quark-gluon plasma and its investigation in central collisions, the particle production will be of interest not only for central but especially in peripheral collisions [1,2], where the two nuclei are assumed to exhibit no overlap. Furthermore, the strong electromagnetic fields associated with the relativistic nuclei should also be regarded as a source for a large dilepton production yield [3–6].

As an additional effect we consider in this paper the electromagnetic dissociation of nuclei as they pass by each other [7–13]. The sudden electromagnetic pulse accompanying the fast impinging nucleus may lead to the dissociation of the collision partner. A recent proton-photoabsorption experiment at HERA [14] indicates that the inelastic  $\gamma p$  cross section rises again for photon energies larger than about 50 GeV in the proton rest frame caused by the hadronic structure of the photon. This increase might contribute considerably to the nuclear electromagnetic dissociation cross section, which has not been taken into account in previous calculations and which could also substantially reduce the proposed luminosities of the aforementioned heavy-ion colliders.

Because of the high collider energies it is justified to utilize the equivalent photon method [1,15]. The strong Lorentz contracted electromagnetic fields of the ultrarelativistic heavy ions can be well simulated by a swarm of equivalent photons. The electromagnetic dissociation of nucleus  $A$  is determined by the equivalent photon spectrum  $n_B(\omega, b)$  of nucleus  $B$ , multiplied with the photon-nucleus dissociation cross section  $\sigma_{\gamma A}(\omega)$ . For the com-

putation of the total cross section we have to integrate over all photon energies  $\omega$  and impact parameters  $b$ :

$$\sigma_{\text{dis}} = \int_{b \geq R_{12}} db 2\pi b \int d\omega n_B(\omega, b) \sigma_{\gamma A}(\omega) \quad (1)$$

Since we only deal with peripheral collisions in order to avoid any direct hadronic interactions, we perform the impact-parameter integration from the sum of the nuclear radii  $R_{12} = R_A + R_B$  up to infinity.

The expression for the equivalent photon distribution can be derived by equating the energy flux of the transverse electromagnetic field of the fast nucleus  $B$  being described by the Poynting vector with the corresponding energy flux of a number of photons. It results [1]

$$n(\omega, b) = \frac{Z^2 \alpha}{\pi^2 \omega} \left| \int_0^\infty dk_\perp k_\perp^2 \frac{F(k_\perp^2 + \omega^2/\gamma^2)}{k_\perp^2 + \omega^2/\gamma^2} J_1(bk_\perp) \right|^2, \quad (2)$$

which indicates the number of photons with energy  $\omega$  for nuclear trajectories at an impact parameter  $b$ .  $\alpha$  is the fine structure constant,  $Z$  is the nuclear charge number,  $\gamma = (1 - v^2/c^2)^{-1/2}$  is the Lorentz contraction factor, and  $F$  denotes the nuclear charge form factor.  $J_1$  is the Bessel function of order 1. The Lorentz factor  $\gamma$  has to be taken in the rest frame of the collision partner, so that a corresponding Lorentz transformation of the c.m. system of the collider with  $\gamma_{\text{coll}}$  to the rest frame yields

$$\gamma = 2\gamma_{\text{coll}}^2 - 1 \quad (3)$$

For relativistic velocities  $v \approx c$  or  $\gamma \gg 1$  we avoid a decomposition of the electromagnetic field into different multipoles. In Fig. 1 we display the equivalent photon spectrum for RHIC ( $\gamma_{\text{coll}} = 100$ ,  $\gamma = 2 \times 10^4$ ) and LHC ( $\gamma_{\text{coll}} = 3100$ ,  $\gamma = 1.9 \times 10^7$ ) energies for different impact parameters. The spectra fall off rapidly for photon energies  $\omega > \gamma/b$ . This becomes obvious in the limiting case  $\omega \gg \gamma/b$ , where the equivalent photon distribution approximates to [1]

$$n(\omega, b) \approx \frac{Z^2 \alpha}{2\pi} \frac{1}{\gamma b} e^{-2\omega b/\gamma} \quad \left(\omega \gg \frac{\gamma}{b}\right). \quad (4)$$

On the other hand, for low photon energies  $\omega \ll \gamma/b$  the number of photons  $n(\omega, b)$  transforms into

$$n(\omega, b) \approx \frac{Z^2 \alpha}{\pi^2} \frac{1}{\omega b^2} \quad \left(\omega \ll \frac{\gamma}{b}\right). \quad (5)$$

In this region the equivalent photon spectrum is independent of the collider energy and is proportional to  $1/b^2$ . As a major result we note that photons with energies of tens of GeV still exist at a distance of about  $1 \text{ \AA}$ .

For the photon-nucleus cross section  $\sigma_{\gamma A}(\omega)$  of  $^{208}\text{Pb}$  we adopt measured data [16]. The largest contribution emerges from the excitation of the giant dipole resonance ( $6 \text{ MeV} \leq \omega \leq 40 \text{ MeV}$ ) [17], which predominantly leads to neutron emission. With increasing photon energy it follows the quasideuteron region [18] and the  $\Delta$ -resonance region [19,20] ( $40 \text{ MeV} \leq \omega \leq 2 \text{ GeV}$ ). High-energy photon-nucleus cross sections are measured up to  $\omega = 80 \text{ GeV}$  for  $^{208}\text{Pb}$  [21–23]. This is exemplified in Fig. 2, where we plot  $\sigma_{\gamma A}(\omega)$  for  $^{208}\text{Pb}$  divided by the nuclear mass number  $A$ . In Table I we present the calculated contributions to the total cross section  $\sigma_{\text{dis}}$  of Eq. (1) from the three different photon energy regions, 6–40 MeV, 40–2000 MeV, and 2–80 GeV. As expected,

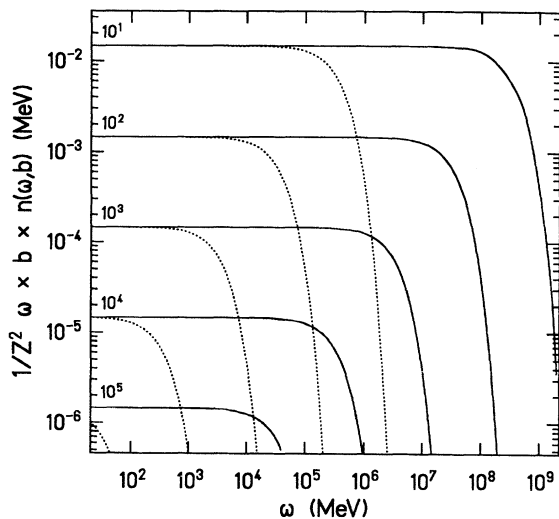


FIG. 1. Equivalent photon distribution  $n(\omega, b)$  for RHIC ( $\gamma = 2 \times 10^4$ , dotted line) and LHC ( $\gamma = 1.9 \times 10^7$ , solid line) energies in dependence on the photon energy  $\omega$  for various impact parameters  $b$ , which is indicated in units of fermi.

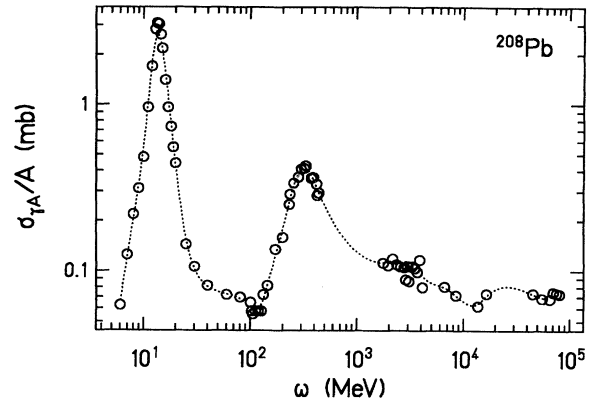


FIG. 2. Measured total photon absorption cross section of  $^{208}\text{Pb}$  divided by the nuclear mass number  $A = 208$  in dependence on the photon energy  $\omega$ . The dotted line depicts the employed interpolation.

the dominant portion originates from the giant resonance region.

For photon energies  $\omega > 80 \text{ GeV}$  no experimental data for  $\sigma_{\gamma \text{Pb}}$  are available, so that we have to extrapolate  $\sigma_{\gamma A}(\omega)$  up to  $\omega \approx \gamma/R$ . At these high energies the photon does not interact purely electromagnetically with the nucleus but also by its hadronic structure [24] resulting from vacuum fluctuation of the photon such as  $\gamma \rightarrow \pi^+ \pi^-$ ,  $\rho$ ,  $\omega$ ,  $\phi$ ,  $q\bar{q}$ ,  $q\bar{q}g$ , etc. For an excellent report we refer to [25]. For this extrapolation purpose we utilize the proton photoabsorption cross section, which has been measured extensively for  $\omega \leq 200 \text{ GeV}$  and which recently has been extended at HERA up to  $\omega \approx 20 \text{ TeV}$  [14]. As a first prescription we employ the extrapolation [25,26] for the electromagnetic dissociation cross section of  $^{208}\text{Pb}$ ,

$$\sigma_{\gamma A} = A_{\text{eff}} \sigma_{\gamma p} = C + D \ln^2 \left( \frac{\omega}{\omega_0} \right). \quad (6)$$

The constant  $C$  is identified with the measured photoabsorption cross section for Pb at  $\omega_0 = 80 \text{ GeV}$ , i.e.,  $C = \sigma_{\gamma \text{Pb}}^{\text{exp}}(\omega = 80 \text{ GeV}) = 15.2 \text{ mb} = A_{\text{eff}} \sigma_{\gamma p}^{\text{exp}}(\omega = 80 \text{ GeV})$ . This also fixes the effective mass number to  $A_{\text{eff}} = 0.65A \approx A^{0.92}$ , which has been introduced to account for nuclear shadowing [27]. As a second extrapolation scheme we also apply the proposed fit [14] to all measured large  $\omega$  inelastic  $\gamma p$  cross sections and multiply it with the effective mass number:

$$\sigma_{\gamma A} = A_{\text{eff}} \left( X s^\epsilon + Y s^{-\eta} \right). \quad (7)$$

TABLE I. Contributions from various photon energy ranges to the dissociation cross section  $\sigma_{\gamma \text{Pb}}$  in a peripheral Pb+Pb collision as calculated from Eq. (1).  $\Sigma$  indicates the sum from the different ranges.

$\gamma_{\text{coll}}$	$\sigma_{\text{dis}}$ (b)			$\Sigma$
	(6–40) MeV	(40–2000) MeV	(2–80) GeV	
100	77.6	25.7	5.6	108.9
3100	133.6	53.7	18.7	206.0
8000	149.1	61.5	22.3	232.9

$s \approx 2M_p\omega$  is the c.m. energy in the  $\gamma p$  system, where  $M_p$  denotes the proton mass and the parameters  $\varepsilon$ ,  $\eta$ ,  $X$ ,  $Y$  are  $\varepsilon = 0.0808$ ,  $\eta = 0.4525$  [14],  $X = 0.06 \text{ mb/GeV}^2$ , and  $Y = 0.16 \text{ mb/GeV}^2$ . In Fig. 3 we present the photon absorption cross section of  $^{208}\text{Pb}$  divided by the nuclear mass number  $A = 208$  in dependence on the photon energy  $\omega$  due to the hadronic structure of the high-energy photon. We have to emphasize that the two data points represent the only measured photon-proton cross sections beyond  $\omega = 200 \text{ GeV}$  multiplied with  $A_{\text{eff}}/A$ . They correspond to  $D \approx 0.2 \text{ mb}$  for the parametrization (6) and the dotted line represents the proposed fit (7). In view of the equivalent photon distributions as displayed in Fig. 1 one may conclude that these extrapolations are rather reliable for RHIC energies, since  $\omega_{\text{max}} \approx \gamma/R \approx 550 \text{ GeV} \ll \omega_{\text{exp}}^{\text{max}} = 20 \text{ TeV}$ . For LHC energies we find  $\omega_{\text{max}} \approx 520 \text{ TeV}$ , which is already by about an order of magnitude larger than  $\omega_{\text{exp}}^{\text{max}}$ . For SSC energies ( $\gamma_{\text{coll}} = 8000$ ,  $\gamma = 1.28 \times 10^8$ ) the extrapolation might not be as justified as for RHIC energies, because  $\omega_{\text{max}} \approx 3500 \text{ TeV} \gg \omega_{\text{exp}}^{\text{max}}$ . Partly motivated by these uncertainties, we also consider the more extreme parametrization (6) with  $D = 0, 0.05, 0.5$ , and  $5 \text{ mb}$ , respectively.

A second effect has to be accounted for in order to calculate properly the total dissociation cross section including also high-energy photons. In Eq. (1) we applied lowest-order perturbation theory which may violate unitarity conservation, because the probability

$$P(b) = \int d\omega n_B(\omega, b) \sigma_{\gamma A}(\omega) \quad (8)$$

formally may exceed its maximum value 1. Unitarity

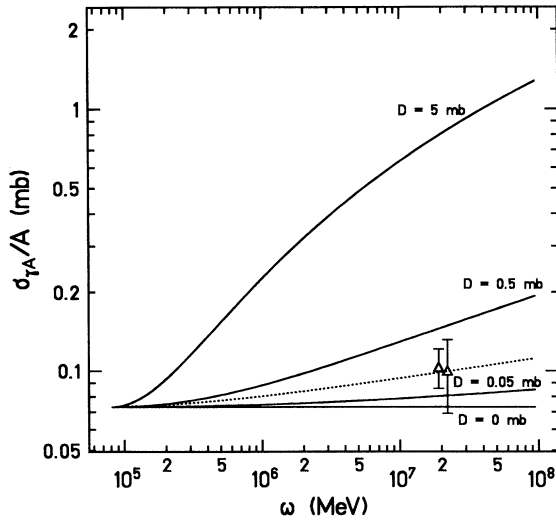


FIG. 3. Total photon absorption cross section of  $^{208}\text{Pb}$  divided by the nuclear mass number  $A = 208$  in dependence on the photon energy  $\omega$ . The two data points at  $\omega \approx 20 \text{ TeV}$  represent measured inelastic  $\gamma p$  cross sections [14] rescaled with the factor  $A_{\text{eff}}/A = 0.65$ . For  $\omega > 80 \text{ GeV}$  the dotted curve represents the extrapolation (7). The solid curves display the parametrization (6) with  $D = 0, 0.05, 0.5$ , and  $5 \text{ mb}$ , respectively.

conservation would be restored by taking into account higher-order corrections. Whenever probabilities larger than one occur, which, e.g., could reflect multiphoton dissociation, we reduce it to its maximum value and the nucleus is assumed to be dissociated. For our consideration it is sufficient to know that the Pb nucleus will definitely be lost for the further beam track. Figure 4 depicts the probability  $P(b)$  in dependence on the impact parameter  $b$  for Pb+Pb collisions at LHC energies for different parametrizations. Unitarity violation occurs for small impact parameters up to  $25 \text{ fm}$  depending on the extrapolation of  $\sigma_{\gamma A}$  for  $\omega > 80 \text{ GeV}$ . The solid line results from the parametrization (7). To obtain the upper dashed curve we used (6) with  $D = 5 \text{ mb}$  and for the lower dashed curve we restricted  $\sigma_{\gamma A}(\omega)$  to the available experimental data up to  $80 \text{ GeV}$ . Even if we neglect completely the high-energy photon contribution, unitarity would be violated in the total Coulomb dissociation cross section. The maximum at about  $7 \text{ fm}$  traces back to the equivalent photon distribution  $n(\omega, b)$ , which yields its largest contribution at the distance of the nuclear radius. Smaller impact parameters lead again to a reduction of  $P(b)$  because of the employed form factor and the associated decrease of the electromagnetic field strength inside the nucleus.

Even very large impact parameters contribute to the total cross section, which is the integral of the dissociation probability  $P(b)$  over  $2\pi b db$ :

$$\sigma_{\text{dis}} = \int_{b \geq R_{12}}^{\infty} db 2\pi b P(b) \quad (9)$$

The approximate  $1/b^2$  decline of  $P(b)$  is partly compen-

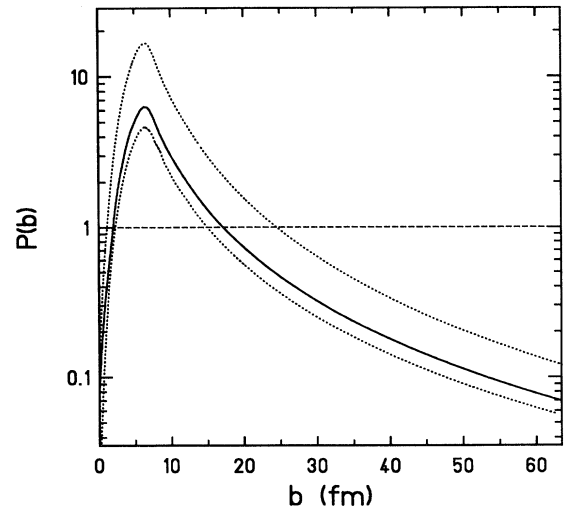


FIG. 4. Nuclear dissociation probability  $P(b)$  in dependence on the impact parameter  $b$  for Pb+Pb collisions at LHC energies ( $\gamma = 3100$ ). The solid curve results from the parametrization (7) whereas the upper dashed line has been obtained using the parametrization (6) with  $C = 15.2 \text{ mb}$ ,  $D = 5 \text{ mb}$ . For the lower dashed line we simply fixed  $C = D = 0$ . Also indicated is the maximum value 1 for the probability  $P(b)$ .

sated by the area element  $2\pi b db$ . Thus the impact-parameter dependence in Eq. (8) is determined by the photon distribution  $n(\omega, b)$ , which reduces to Eq. (5) for not too large  $\omega b/\gamma$ . In this range the photon spectrum is independent of  $\gamma$  and covers completely the region of available experimental data. Therefore  $P(b)$  displays a  $1/b^2$  dependence up to about  $10^5$  fm for RHIC energies. For still larger impact parameters the photon spectrum (4) declines rapidly.

We also evaluate  $\sigma_{\text{dis}}^{\text{uni}}$ , where we use as an upper limit  $P(b) = 1$  in Eq. (9). The computed cross sections are listed in Table II, where “no”  $D$  factor means that the integration over  $\omega$  is restricted to the experimental Pb data up to 80 GeV and “other,” that we employ the extrapolation (7). One can deduce from Table II that unitarity violation plays practically no role for RHIC energies. For LHC and SSC energies the difference between the cross section (1) and its simple unitarized version becomes large only if the extrapolations for  $\sigma_{\gamma A}$  ( $\omega > 80$  GeV) are extremely enhanced ( $D = 5$  mb), which, however, is not supported by experimental data. Using the extrapolation of Eq. (7) we derived the following results for the unitarized Coulomb dissociation cross section of Pb in a Pb+Pb collision: for RHIC energies we find  $\sigma_{\text{dis}}^{\text{uni}}(\text{other}) = 108.9$  b, for LHC energies we obtain  $\sigma_{\text{dis}}^{\text{uni}}(\text{other}) = 221.7$  b, and for SSC energies we calculated  $\sigma_{\text{dis}}^{\text{uni}}(\text{other}) = 258.3$  b.

These refined calculations of the Coulomb dissociation cross section imply some immediate consequences for the heavy-ion collider luminosities. For RHIC the influence of the hadronic photon structure for photon energies greater than the measured 80 GeV turns out to be negligible, so that the expected luminosity does not diminish. For LHC the situation is different; our calculated cross sections for the Coulomb dissociation process in a Pb+Pb collision is about 40 b larger than a previous calculation [7], which modifies the expected luminosity.

In principle, the Coulomb dissociation process could be used as a trigger on the impact parameter. For very large impact parameters only relatively small photon energies contribute, so that the dissociation process corresponds mainly to a neutron emission caused by the ex-

TABLE II. The dissociation cross section  $\sigma_{\text{dis}}$  and  $\sigma_{\text{dis}}^{\text{uni}}$ ; for the latter we adopt the probability restriction to 1. “No”  $D$  factor means that we use only the experimental data for the photon-nucleus cross section up to  $\omega = 80$  GeV, and “other” means that we use the extrapolation indicated in Eq. (7).

$\gamma_{\text{coll}}$	$D$ factor (mb)	$\sigma_{\text{dis}}$ (b)	$\sigma_{\text{dis}}^{\text{uni}}$ (b)
100	No	108.9	108.9
	0	108.9	108.9
	0.05	108.9	108.9
	0.5	108.9	108.9
	5	109.1	109.0
	Other	108.9	108.9
3100	No	206.0	205.9
	0	220.4	219.8
	0.05	221.0	220.3
	0.5	225.4	224.3
	5	270.3	260.6
	Other	222.3	221.7
8000	No	232.9	232.7
	0	255.0	254.3
	0.05	256.2	255.4
	0.5	266.7	264.9
	5	372.1	348.2
	Other	259.2	258.3

citation of the giant resonance. In contrast to this the hadronic structure of the photon becomes more and more important for very small impact parameters. Part of the nuclear fragmentation can be generated by an incoming gluon or quark leading to strong interaction processes inside the nucleus and finally to fragmentation. The nucleus might be dissociated into more or less independent hadrons, which could be detected in the spectator detector at large rapidities.

We are grateful for fruitful conversations with U. Kneissl, D. Brandt, H. Gutbrod, J. Schukraft, N. Baron, and G. Baur. One of us (M.G.) wants to thank the Alexander von Humboldt Stiftung for its support.

- 
- [1] M. Vidović, M. Greiner, C. Best, and G. Soff, Phys. Rev. C **47**, 2308 (1993).  
[2] M. Greiner, M. Vidović, and G. Soff, Phys. Rev. C **47**, 2288 (1993).  
[3] C. Best, W. Greiner, and G. Soff, Phys. Rev. A **46**, 261 (1992).  
[4] N. Baron and G. Baur, Phys. Rev. D **46**, R3695 (1992).  
[5] G. Baur, Z. Phys. C **54**, 419 (1992).  
[6] G. Soff, D. Hilberg, Ch. Hofmann, Ch. Best, S. Schneider, M. Vidović, and M. Greiner, Rev. Mex. Fis. **38**, 196 (1992).  
[7] G. Baur and C.A. Bertulani, Nucl. Phys. **A505**, 835 (1989).  
[8] J.W. Norbury, Phys. Rev. C **43**, R368 (1991).  
[9] J.W. Norbury, Phys. Rev. C **47**, 406 (1993).  
[10] Th. Frommhold, F. Steiper, W. Henkel, U. Kneissl, J. Ahrens, R. Beck, J. Peise, and M. Schmitz, Phys. Lett. B **295**, 28 (1992).  
[11] D.I. Ivanov, G.Ya. Kezerashvili, V.G. Nedorezov, A.S. Sudov, and A.A. Turinge, Yad. Fiz. **55**, 2623 (1992) [Sov. J. Nucl. Phys. **55**, 1464 (1992)].  
[12] R. Fleischhauer and W. Scheid, Nucl. Phys. **A510**, 817 (1990).  
[13] T. Aumann, J.V. Kratz, E. Stiel, K. Sümmerer, W. Brühlle, M. Schädel, G. Wirth, M. Fauerbach, and J.C. Hill, Phys. Rev. C **47**, 1728 (1993).  
[14] G. Wolf, Phys. Lett. B **293**, 465 (1993).  
[15] C. A. Bertulani and G. Baur, Phys. Rep. **163**, 299 (1988).  
[16] J. Ahrens, Nucl. Phys. **A446**, 229c (1985).  
[17] B.L. Berman and S.C. Fultz, Rev. Mod. Phys. **47**, 713 (1975).  
[18] A. Lepretre, H. Beil, R. Bergere, P. Carlos, J. Fagot,

- A. De Miniac, and A. Veyssiere, Nucl. Phys. **A367**, 237 (1981).
- [19] P. Carlos, H. Beil, R. Bergere, J. Fagot, A. Lepretre, A. De Miniac, and A. Veyssiere, Nucl. Phys. **A431**, 573 (1984).
- [20] J. Arends, J. Eyink, A. Hegerath, K.G. Hilger, B. Mecking, G. Nöldeke, and H. Rost, Phys. Lett. **98B**, 423 (1981).
- [21] G.R. Brookes *et al.*, Phys. Rev. D **8**, 2826 (1973).
- [22] D.O. Caldwell, V.B. Elings, W.P. Hesse, R.J. Morrison, F.V. Murphy, and D.E. Yount, Phys. Rev. D **7**, 1362 (1973).
- [23] D.O. Caldwell *et al.*, Phys. Rev. Lett. **42**, 553 (1979).
- [24] S.M. Schneider, W. Greiner, and G. Soff, J. Phys. G **19**, L39 (1993).
- [25] W. Weise, Phys. Rep. **13**, 53 (1974).
- [26] E. Leader and U. Maor, Phys. Lett. **43B**, 505 (1973).
- [27] L. Frankfurt and M. Strikman, Phys. Rep. **160**, 235 (1988).